MCB
Journals.ASM.org

Transcriptional Regulation of the Human Tumor Suppressor *DOK1* by E2F1

Maha Siouda, Jiping Yue,* Ruchi Shukla,* Sophie Guillermier,* Zdenko Herceg, Marion Creveaux,* Rosita Accardi, Massimo Tommasino, and Bakary S. Sylla

International Agency for Research on Cancer, Lyon, France

The expression of the tumor suppressor *DOK1* is repressed in a variety of human tumors as a result of hypermethylation of its promoter region. However, the molecular mechanisms by which *DOK1* expression is regulated have been poorly investigated. Here, we show that the expression of *DOK1* is regulated mainly by the transcription factor E2F1. We identified three putative E2F1 response elements (EREs) in the *DOK1* promoter region. E2F1 had a relatively higher binding affinity for the ERE located between bp −498 and −486 compared with the other two EREs. E2F1 gene silencing strongly inhibited *DOK1* expression. E2F1-driven *DOK1* transcription occurred in the presence of cellular stresses, such as accumulation of DNA damage induced by etoposide. *DOK1* silencing promoted cell proliferation and protected against etoposide-induced apoptosis, indicating that DOK1 acts as a key mediator of cellular stress-induced cell death. Most importantly, we observed that DNA methylation of the *DOK1* core promoter region found in head and neck cancer cell lines hampered the recruitment of E2F1 to the *DOK1* promoter and compromised *DOK1* expression. In summary, our data show that E2F1 is a key factor in *DOK1* expression and provide novel insights into the regulation of these events in cancer cells.

Genetic alterations of tumor suppressor genes, such as gene mutations or silencing of gene expression through aberrant epigenetic modifications (e.g., DNA methylation), are frequent events in a wide variety of human cancers (3). DOK1 (*d*ownstream *o*f tyrosine *k*inase *1*), first identified as an abundant tyrosine-hyperphosphorylated protein in chronic myelogenous leukemia (CML) cells (5), belongs to a large family of phosphotyrosine adapters (DOK), which share significant parity with the insulin receptor substrates (IRS) (18). So far, seven members (DOK1 to DOK7) have been identified and found to be implicated in the regulation of multiple biological processes, including cell growth, transformation, death, motility, and differentiation (18, 19).

DOK1 displays tumor suppressor effects as it inhibits cell proliferation, downregulates mitogen-activated protein (MAP) kinase activity, opposes leukemogenesis, and promotes cell spreading, motility, and apoptosis (8, 10, 31–33). In addition, the *DOK1* gene locus is localized in human chromosome 2p13, which is frequently rearranged in various human tumors (11, 22, 34). Indeed, we reported a frameshift mutation of the *DOK1* gene in chronic lymphocytic leukemia (CLL), resulting in truncated DOK1 found exclusively in the nucleus, in contrast to the cytoplasmic wild-type protein (16). Consistent with these findings, we discovered that DOK1 harbors a nuclear exclusion site (NES) that allows it to shuttle between the cytoplasm and the nucleus (16). Interestingly, a constitutive nuclear DOK1-NES mutant was found to be defective in its abilities to inhibit cell proliferation and promote cell spreading (16). This raises the possibility that the subcellular localization of DOK1 regulates its functions (16). Additional evidence for the tumor suppressor effects of DOK1 came from animal studies. *DOK1* or *DOK2* knockout mice show a high susceptibility to developing leukemia and hematological malignancies (19, 23, 33), as well as lung adenocarcinomas (2). Concomitant with these findings, we showed that *DOK1* gene expression was repressed in a large proportion of head and neck cancer (HNC), lung, liver, and gastric cancers, and Burkitt's lymphoma as a result of aberrant hypermethylation of the *DOK1* promoter region (1, 14, 24). These data firmly establish the tumor suppressor properties of *DOK1*. Given that *DOK1* is frequently altered in a variety of human cancers, it could potentially serve as a new marker and/or a therapeutic target for cancer control (1, 2, 14, 24).

Because DNA methylation is thought to impair the transcriptional machinery at the promoter region, thus hampering gene transcription, it is of interest to characterize the *cis* elements and the transcription factors that regulate *DOK1* gene expression, particularly in the context of its potential role in tumor initiation and progression. However, very little is known about cellular transcription factors involved in the regulation of the *DOK1* promoter.

In this study, we characterized the *DOK1* promoter region and identified E2F1, a key factor in the control of the cell cycle and proliferation (6, 7), as a transcription factor that plays a pivotal role in regulating *DOK1* gene expression.

MATERIALS AND METHODS

Plasmids, cloning, and mutagenesis. The region 2.0 kb upstream of the *DOK1* initiation site was cloned by PCR from genomic DNA into the pGL3 luciferase reporter (Promega) to generate pGL3.*DOK1*-1. The de-

Received 1 August 2012 Returned for modification 31 August 2012
Accepted 27 September 2012
Published ahead of print 1 October 2012

Address correspondence to Bakary S. Sylla, syllab@iarc.fr.

* Present address: Jiping Yue, The Ben May Department for Cancer Research, University of Chicago, Chicago, Illinois, USA; Ruchi Shukla, Genetics and Genomics Division, Roslin Institute, University of Edinburgh, Easter Bush, Midlothian, Scotland, United Kingdom; Sophie Guillermier, MERIAL, Lyon, France; Marion Creveaux, CRCL, Équipe Apoptose, Cancer et Développement, Lyon Cedex, France.

Supplemental material for this article may be found at http://mcb.asm.org/.

doi:10.1128/MCB.01050-12

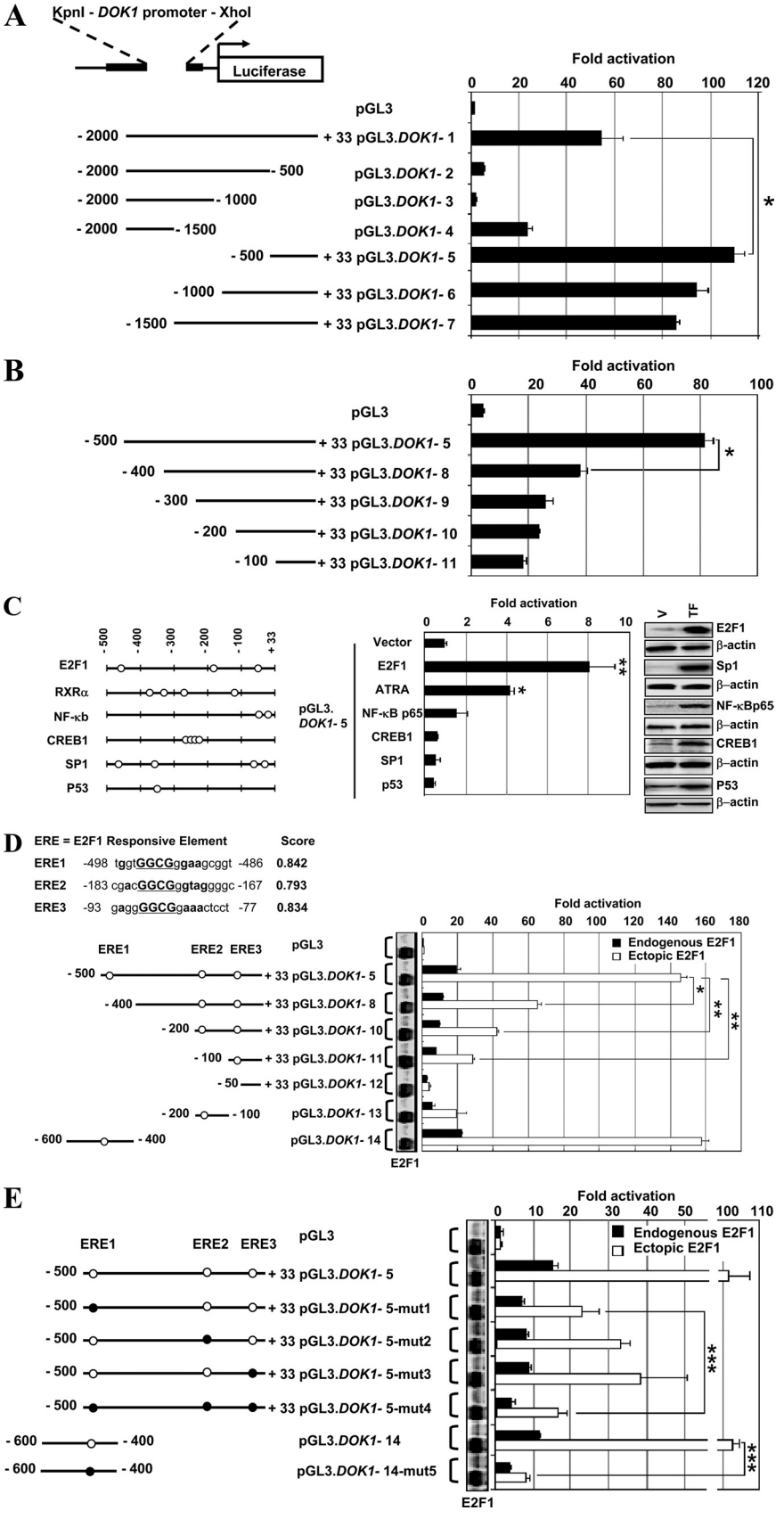
A
KpnI - DOK1 promoter - XhoI
Luciferase
Fold activation
pGL3
- 2000 + 33 pGL3.DOK1- 1
- 2000 - 500 pGL3.DOK1- 2
- 2000 - 1000 pGL3.DOK1- 3
- 2000 - 1500 pGL3.DOK1- 4
- 500 + 33 pGL3.DOK1- 5
- 1000 + 33 pGL3.DOK1- 6
- 1500 + 33 pGL3.DOK1- 7
B
Fold activation
pGL3
- 500 + 33 pGL3.DOK1- 5
- 400 + 33 pGL3.DOK1- 8
- 300 + 33 pGL3.DOK1- 9
- 200 + 33 pGL3.DOK1- 10
- 100 + 33 pGL3.DOK1- 11
C
E2F1
RXRα
NF-κb
CREB1
SP1
P53
pGL3. DOK1- 5
Fold activation
Vector
E2F1
ATRA
NF-κB p65
CREB1
SP1
p53
TF
E2F1
β-actin
Sp1
NF-κBp65
CREB1
P53
D
ERE = E2F1 Responsive Element Score
ERE1 -498 tggtGGCGggaagcggt -486 0.842
ERE2 -183 cgacGGCGggtaggggc -167 0.793
ERE3 -93 gaggGGCGgaaactcct -77 0.834
Fold activation
Endogenous E2F1
Ectopic E2F1
ERE1 ERE2 ERE3 pGL3
- 500 + 33 pGL3.DOK1- 5
- 400 + 33 pGL3.DOK1- 8
- 200 + 33 pGL3.DOK1- 10
- 100 + 33 pGL3.DOK1- 11
- 50 + 33 pGL3.DOK1- 12
- 200 - 100 pGL3.DOK1- 13
- 600 - 400 pGL3.DOK1- 14
E2F1
E
Fold activation
Endogenous E2F1
Ectopic E2F1
ERE1 ERE2 ERE3 pGL3
- 500 + 33 pGL3.DOK1- 5
- 500 + 33 pGL3.DOK1- 5-mut1
- 500 + 33 pGL3.DOK1- 5-mut2
- 500 + 33 pGL3.DOK1- 5-mut3
- 500 + 33 pGL3.DOK1- 5-mut4
- 600 - 400 pGL3.DOK1- 14
- 600 - 400 pGL3.DOK1- 14-mut5
E2F1

letion mutants pGL3.*DOK1*-2 to pGL3.*DOK1*-15 (Fig. 1) were generated by PCR from pGL3.*DOK1*-1 using primers with XhoI (CTCGAG) and KpnI (GGTACC) sites at the 5′ and 3′ end, respectively, and inserted into pGL3 (see Table S1A in the supplemental material). Mutations of putative E2F1 response elements (EREs) in the *DOK1* promoter were generated using the QuikChange Lightning site-directed mutagenesis kit (Stratagene) using ERE-specific primers (see Table S1B in the supplemental material). The sequence of the inserts was confirmed by sequencing. The pCMV-E2F1 and pCMV-E2F1 (amino acids [aa] 1 to 374) plasmids were obtained from Kristian Helin (University of Copenhagen, Denmark). pcDNA3-p65 was obtained from Tom Gilmore (Boston University), and the pN3-SP1 plasmid was obtained from Guntram Suske (Philipps University Marburg, Germany). The CREB1 plasmid has been described previously (36), and p53 was obtained from Pierre Hainaut (IARC, France). The *Renilla* construct was obtained from BD Clontech.

Database search for transcription factor response elements. The *DOK1* promoter sequence 2.0 kb upstream of the *DOK1* ATG site was analyzed by searching the Genomatix MatInspector database using the Matrix Family Library version 8.1 for general core promoter elements in vertebrates and a fixed matrix similarity threshold of 0.75. Putative E2F response elements and their respective consensus sequences and locations are given in Table S1C in the supplemental material.

Cells, transfection, and chemicals. HEK293 cells and the HNC cell lines HNC-41 (tonsil), HNC-97 (oral cavity), HNC-124 (oral cavity), and PNS-136 (paranasal sinus) and the colon cancer cell line LoVo were described previously (24). HEK293 cells were transfected using Fugene 6 (Roche Diagnostics) and analyzed 48 h after transfection. For treatment, cells were incubated in medium containing different reagents: 25, 50, or 100 μM etoposide (Sigma) in dimethyl sulfoxide (DMSO) for 24 h or 0.3 μM all-*trans* retinoic acid (ATRA) (R2625; Sigma) in ethanol for 48 h. Inhibition of DNA methylation was performed by using 5′-aza-2′-deoxycytidine (5′-aza) at 30 μM (Sigma) dissolved in DMSO for 4 days, and cells were then harvested for analysis.

Reporter assays. Cells were transfected with 0.250 μg of pGL3 or *DOK1* promoter plasmids along with other experimental plasmids using Fugene 6 (Roche Diagnostics). The *Renilla* construct was included for normalization of transfection efficiency. At 48 h after transfection, cells were harvested and the enzyme activities of firefly and *Renilla* luciferase were measured using the Dual-Luciferase reporter assay system (Promega). The luminescence signal was quantified using an Optocomp I luminometer (MGM Instruments). Each condition was used in triplicate and replicated in different independent experiments.

Gene silencing. Small interfering RNAs (siRNA) to knock down E2F1 (si-E2F1) oligonucleotides (sense, GGCCCGAUCGAUGUUUUCC, and antisense, GGAAAACAUCGAUCGGGCC) (Sigma) were used to silence E2F1. siRNA specific for luciferase (si-Luc) (sense, CGUACGCGGAAUA CUUCGAUU, and antisense, UUGCAUGCGCCUUAUGAAGCU) (Ambion) were used as a negative control. siRNA oligonucleotides were transfected into HEK293 cells at 200 nM using Lipofectamine 2000 (Invitrogen). *E2F1* small hairpin RNA (shRNA)-expressing retroviral vectors (TG320325) purchased from OriGene Technologies were used to stably silence E2F1 expression in the HNC cell lines HNC-41 and HNC-124 and the control PNS-136. To inhibit *DOK1* expression, two target sequences for *DOK1* interference, GGATCAAAGAAGATGGTTA and CAGAATGG GTGCAGTTTGA, were cloned as the hairpin structures *DOK1*-shRNA1 and *DOK1*-shRNA2, respectively, under the control of the H1 promoter in the psiHIV-H1 vector (GeneCopoeia) and transduced into the cells. The scramble sequence GAAGATTAAGTGCGATAGA was used as a control.

Antibodies and immunoblotting. The following antibodies were used: anti-DOK1 ab8112 (Abcam), E2F1 sc-56662, E2F1 sc-251x, E2F2 sc-633, E2F3 sc-866 (all from Santa Cruz Biotechnology), β-actin C4 (MP Biomedicals), p53 DO-7 (Novocastra), anti-BAX sc-526, mouse IgG, rabbit IgG (all from Santa Cruz Biotechnology), H3K9ac (Cell Signaling Technology), H3K4me3, and H3K27me3 (both from Epigentek). Immunoblotting was performed as described previously (24).

Quantitative RT-PCR. Total RNA was extracted using TRIzol reagent (Life Technologies). Reverse transcription was performed using the RevertAid H Minus First Strand cDNA synthesis kit (Fermentas) according to the manufacturer's protocol. Real-time PCR (RT-PCR) was performed using gene-specific primers for *DOK1*, *E2F1*, and *GAPDH* (glyceraldehyde-3-phosphate dehydrogenase) (see Table S1D in the supplemental material). Data were analyzed using MxPro software (Stratagene).

Chromatin immunoprecipitation. Cells were cross-linked with 1% formaldehyde, harvested and sonicated to shear chromatin into fragments of 0.2 kb, and then processed according to the standard protocol for chromatin immunoprecipitation (ChIP) analysis using the assay kit from Cell Signaling. The input and immunoprecipitated DNA were then analyzed by real-time PCR using primers for the *DOK1* promoter regions ERE1, ERE2, and ERE3. The region from bp −1180 to −791 of the *DOK1* promoter, with no predicted E2F binding sites, was used as a negative control, and regions from the c-*FOS* and c-*Myc* promoters were used as a positive control (see Table S2A in the supplemental material). Data were calculated as percentage of enrichment of input.

Transient-transfection ChIP assay. HEK293 cells were transfected with pGL3 constructs harboring different regions of the *DOK1* promoter containing only a single ERE (wild-type or mutated). At 48 h after transfection, the cells were harvested by cross-linking with 1% formaldehyde, lysed in RSB buffer (3 mM $MgCl_2$, 10 mM NaCl, 10 mM Tris-HCl at pH 7.4, and 0.1% Igepal CA-630) instead of normal cell lysis buffer, and further processed using the standard ChIP protocol.

DNA pulldown assay. DNA pulldown assays were carried out as described by Gong et al. (9). Cells were lysed by sonication in HKMG buffer (10 mM HEPES at pH 7.9, 100 mM KCl, 5 mM $MgCl_2$, 10% glycerol, 1

FIG 1 E2F1 is a major transcription factor activating the *DOK1* promoter. HEK293 cells were cotransfected together with the *Renilla* plasmid (used as an internal control for transfection) and with the indicated pGL3-based reporter constructs containing different deletion mutants of the *DOK1* promoter: pGL3.*DOK1*-1 to -7 (A) or pGL3.*DOK1*-5 and -8 to -11 (B). After 48 h, luciferase activity was measured. Results (mean ± standard deviation [SD]) are representative of three independent experiments performed in triplicate. Luciferase fold induction is expressed relative to the baseline luciferase activity of pGL3 basic vector. Data were analyzed using Student's *t* test (*, $P < 0.05$). (C) The sequence of the 0.5-kb region upstream of the *DOK1* ATG site was analyzed for the presence of transcription factor response elements by searching the Genomatix MatInspector database. Black lines represent the DNA sequence, and white circles represent different indicated transcription factor binding sites. HEK293 cells were cotransfected with pGL3 basic or the pGL3.*DOK1*-5 promoter reporter construct along with the empty vector (V) or expression plasmids for transcription factors (TF) (pCMV-E2F1, pcDNA3-p65, pNI-Creb1, pN3-Sp1, and pcDNA3-p53) or stimulated with ATRA, which induces the activation of RXR factors. Luciferase activity was measured 48 h after transfection. Results (mean ± SD) are representative of three independent experiments performed in triplicate. Luciferase fold induction is expressed relative to the baseline luciferase activity of control vector. The expression of transcription factors was verified by immunoblotting. (D) Consensus sequences of EREs within the *DOK1* promoter. The underlined capital letters denote the core sequence, and the bold letters appear in a position where the matrix exhibits a high conservation profile (confidence interval, >60). The scores represent the matrix similarity calculated using the MatInspector algorithm. HEK293 cells were cotransfected with the deletion mutant of the *DOK1* promoter pGL3.*DOK1*-5, -8, and -10 to -14 or pGL3.*DOK1*-5, E2F1-binding-site-mutated constructs pGL3.*DOK1*-5-mut1 to -mut4, pGL3.*DOK1*-14, or pGL3.*DOK1*-14-mut5 (E), along with empty vector pCMV (endogenous E2F1, black bars) or expression pCMV-E2F1 (ectopic E2F1, white bars). At 48 h after transfection, luciferase activity was measured. Results (mean ± SD) are representative of three independent experiments performed in triplicate. Data were analyzed using Student's *t* test (*, $P < 0.05$; **, $P < 0.01$; ***, $P < 0.001$). White circles represent the wild-type sequence of ERE1, ERE2, and ERE3 in the promoter region, whereas black circles represent mutants of ERE1, ERE2, and ERE3, obtained by replacing the core GGCG of the consensus sequence with AAAA.

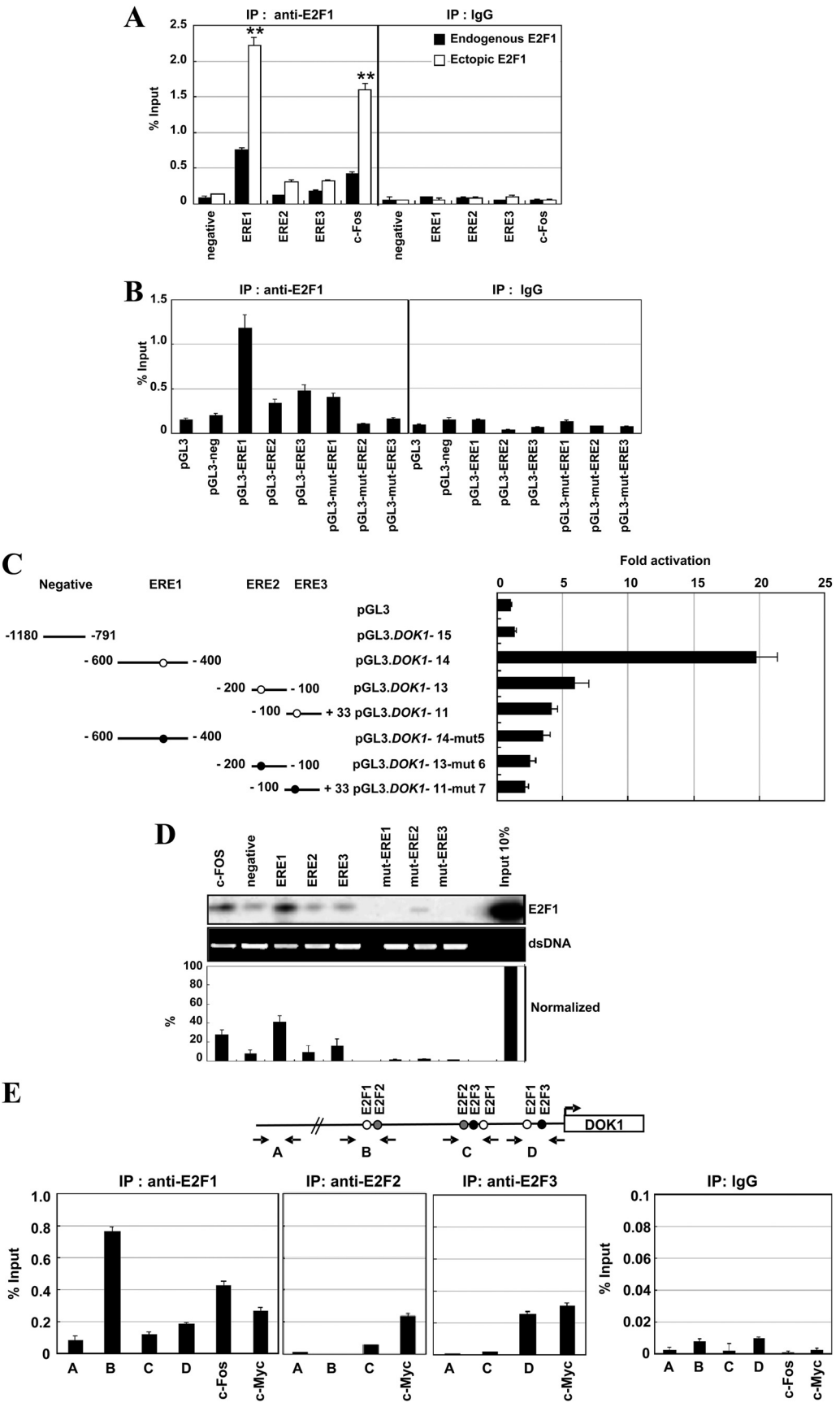
A
IP : anti-E2F1
IP : IgG
Endogenous E2F1
Ectopic E2F1
% Input
negative
ERE1
ERE2
ERE3
c-Fos
B
IP : anti-E2F1
IP : IgG
% Input
pGL3
pGL3-neg
pGL3-ERE1
pGL3-ERE2
pGL3-ERE3
pGL3-mut-ERE1
pGL3-mut-ERE2
pGL3-mut-ERE3
C
Negative
ERE1
ERE2
ERE3
Fold activation
-1180 -791
- 600 - 400
- 200 - 100
- 100 + 33
pGL3
pGL3.DOK1- 15
pGL3.DOK1- 14
pGL3.DOK1- 13
pGL3.DOK1- 11
pGL3.DOK1- 14-mut5
pGL3.DOK1- 13-mut 6
pGL3.DOK1- 11-mut 7
D
c-FOS
negative
ERE1
ERE2
ERE3
mut-ERE1
mut-ERE2
mut-ERE3
Input 10%
E2F1
dsDNA
Normalized
%
E
E2F1 E2F2
E2F2 E2F3 E2F1
E2F1 E2F3
DOK1
A
B
C
D
IP : anti-E2F1
IP: anti-E2F2
IP: anti-E2F3
IP: IgG
% Input
c-Fos
c-Myc

mM dithiothreitol [DTT], and 0.5% NP-40) containing protease and phosphatase inhibitors. Cellular debris was removed by centrifugation. Next, 1 mg of total lysate was precleared with 40 μl of streptavidin-agarose beads (Thermo Scientific) for 1 h at 4°C, with rotation, and incubated with 2 μg of biotinylated PCR product oligonucleotides and 20 μg of poly(dI-dC) for 16 h at 4°C, with rotation. Biotin-oligonucleotide-protein complexes were collected with 60 μl of streptavidin-agarose beads for 1 h at 4°C, with rotation, washed twice with HKMG buffer, separated on SDS-PAGE, and detected by Western blotting. The biotinylated double-stranded oligonucleotides were amplified using the same primers as for ChIP with 5′ biotin.

Stable flow cytometry analysis. HEK293 cells stably expressing the scramble sequence or *DOK1*-shRNA1 or *DOK1*-shRNA2 under the control of the H1 promoter in the psiHIV-H1 vector were generated by transfection using Fugene 6 (Roche Diagnostics) and puromycin (0.5 μg/ml) for selection. The inhibition of *DOK1* expression was monitored by RT-PCR and immunoblotting. The established HEK293 cells were treated with 50 μM etoposide or an equivalent volume of DMSO (mock) for 24 h. Apoptotic cells were detected using the APC annexin V apoptosis detection kit I (BD Pharmingen) according to the manufacturer's instructions. Stained cells were detected using the BD FACSCanto II flow cytometer (BD Biosciences) and analyzed using BD FACSDiva software.

***In vitro* methylation.** Amplified ERE oligonucleotides (see Table S2A in the supplemental material) and the pGL3-*DOK1*-1, -5, and -14 plasmids were treated without (mock) or with CpG methylase M.SssI (NEB) (methylated) according to the manufacturer's instructions and then used for the DNA pulldown and reporter assays, respectively, as described above.

DNA extraction and bisulfite genomic sequencing. Genomic DNA was extracted using the QIAamp DNA minikit (Qiagen) and then treated with bisulfite using the EZ DNA Methylation-Gold kit (Zymo Research). Different EREs were amplified and cloned using the TA cloning kit (Invitrogen). Multiple individual clones were sequenced. Primers for PCR amplification and sequencing are given in Table S2B in the supplemental material.

RESULTS

Identification of the minimal region of the DOK1 gene displaying promoter activity. To characterize the region required for *DOK1* gene expression, we cloned a segment 2.0 kb upstream of the *DOK1* initiation codon in the pGL3 reporter plasmid and evaluated its transcriptional activity. We observed about 60-fold induction of luciferase activity compared with the empty control plasmid (Fig. 1A). To identify the minimal region required for promoter activity, several deletion mutants within the 2.0-kb region were generated and then assessed for their activity. The DNA segment with the highest promoter activity was found to be localized between bp −500 and +33 (Fig. 1A). Further sequential deletions of 100 bp within the 0.5-kb region showed that the region between bp −500 and −400 contains important positive regulatory elements (Fig. 1B).

E2F1 is a major transcription factor regulating *DOK1* promoter activity. Next, we analyzed the sequence of the 0.5-kb region identified above using the Genomatix MatInspector database to determine the presence of putative transcription factor response elements. The analysis revealed the presence of potential binding sites for several transcription factors, including SP1, P53, E2F family members, CREB, NF-κB, and retinoid X receptors (RXRs) (Fig. 1C, left, and 2E).

To evaluate the involvement of these transcription factors in the regulation of the *DOK1* promoter, we performed luciferase reporter assays using the region between bp −500 and +33 of the *DOK1* gene in HEK293 cells in the absence or presence of the expression plasmids of the transcription factors E2F1, NF-κB, CREB1, SP1, and p53. We also tested the effect of exposure of cells to ATRA, which has been shown to induce *DOK1* gene expression, probably via the engagement of RXRs (15). We found that E2F1 expression induced 8-fold luciferase activity compared with control cells transfected with the empty vector (Fig. 1C, right), whereas treatment with ATRA resulted in 4-fold induction. NF-κB marginally activated the *DOK1* promoter, and some inhibitory effects were observed with CREB1, SP1, and p53 (Fig. 1C, right). Thus, E2F1 and ATRA have a significant positive effect on the *DOK1* promoter, and E2F1 is a major transcription factor inducing *DOK1* promoter activity.

The sequences of the three putative core binding sites of E2F1, referred to as ERE1 (bp −498 to −486), ERE2 (bp −183 to −167), and ERE3 (bp −93 to −77), are shown in Fig. 1D (top) together with their significance scores. To identify which element(s) is functionally required for E2F1-mediated *DOK1* promoter activity, we generated sequential deletions of these elements within the 0.5-kb region and performed the luciferase reporter assay in the presence of endogenous or ectopically expressed E2F1 protein. Deletion of the region containing ERE1 resulted in a reduction of more than 50% in promoter activity in cells expressing endogenous or ectopic E2F1 (Fig. 1D, bottom). The additional deletion of the regions containing ERE2 or ERE3 caused significant, but less pronounced, decreases in *DOK1* promoter activity. In addition,

FIG 2 E2F1 is recruited to the *DOK1* promoter. (A) HEK293 cells were transfected with the empty vector pCMV (endogenous E2F1) or the expression vector pCMV-E2F1 (ectopic E2F1) and then subjected to quantitative ChIP assay using the indicated antibodies. The *DOK1* promoter was amplified by real-time PCR using different primers (see Table S2 in the supplemental material). Data were calculated as percentages of enrichment of input. Error bars indicate the SD from two independent experiments performed in triplicate. (B) HEK293 cells were transfected with the indicated pGL3-*DOK1* promoter constructs containing only a single ERE (wild type or mutated), and 48 h later, a quantitative ChIP assay was performed (see "Transient-transfection ChIP assay" in Materials and Methods) to assess the E2F1 binding *in vivo* to *DOK1* promoter EREs. The input as the immunoprecipitated *DOK1* promoter fragment inserted in pGL3 vector was amplified by real-time PCR using pGL3 primers flanking each insert. Error bars indicate the SD from two independent experiments performed in triplicate. (C) The promoter activity of the indicated ERE was evaluated as described for Fig. 1A. Results (mean ± SD) are representative of two independent experiments in triplicate. (D) *In vitro* DNA pulldown assay. PCR products, using the same primers as described for panel A, but 5′ biotinylated, were incubated with total lysate from E2F1-overexpressing HEK293 cells and then pulled down using streptavidin-agarose beads. Immunoblotting was used to check the recruitment of E2F1 to the different PCR fragments. E2F1 protein bands from three independent experiments were quantified using ImageJ software, and the values were normalized to the PCR products used in each experiment and checked on an agarose gel (double-stranded DNA) (bottom). (E) HEK293 cells were subjected to quantitative ChIP assay using the indicated antibodies. The *DOK1* promoter was amplified by real-time PCR using different primers (see Table S2). Region A from bp −1180 to −791 of the *DOK1* promoter that lacks putative binding sites for E2Fs was used as negative control, the binding site in the c-*FOS* promoter was used as a positive control for E2F1 recruitment, and the c-*Myc* promoter was used for E2F1, E2F2, and E2F3 binding. Region B of the *DOK1* promoter contains the putative binding sites for E2F1 (ERE1, bp −498 to −486) and E2F2 (bp −451 to −435). Region C contains the putative binding sites for E2F1 (ERE2, bp −183 to −167), E2F2 (bp −252 to −235), and E2F3 (bp −218 to −201). Region D contains the putative binding sites for E2F1 (ERE3, bp −93 to −77) and E2F3 (bp −45 to −28). Data are presented as percentages of input. Error bars indicate the SD from two independent experiments performed in triplicate.

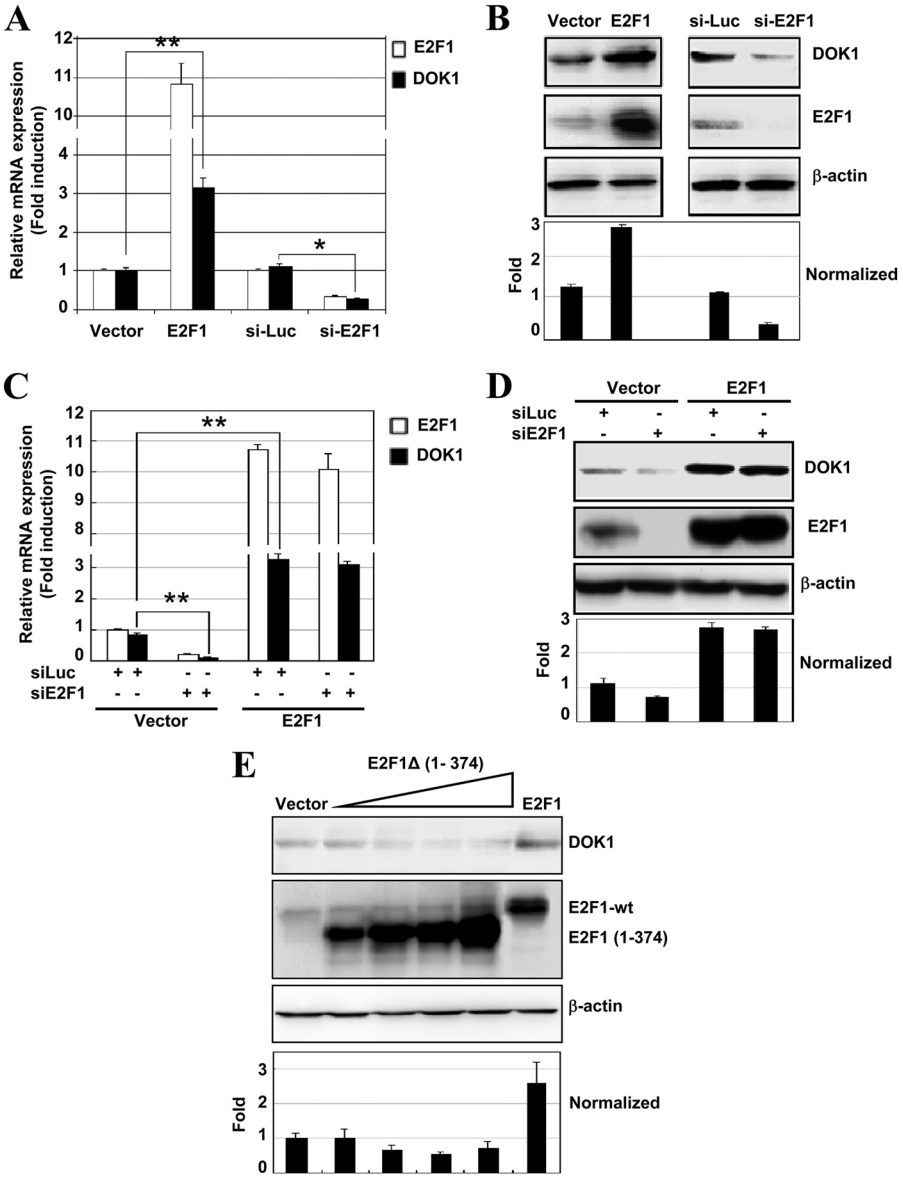

FIG 3 E2F1 induces *DOK1* gene expression. HEK293 cells were transfected with the pCMV empty vector, pCMV-E2F1 constructs, si-E2F1, or si-Luc. (A) The mRNA expression levels of *E2F1* and *DOK1* were monitored by quantitative RT-PCR. Values were normalized to the expression level of the housekeeping gene *GAPDH* using the threshold cycle ($\Delta\Delta C_T$) method. Fold induction is expressed relative to the baseline si-Luc. Data were analyzed using Student's *t* test (*, $P < 0.05$; **, $P < 0.01$). (B) Immunoblotting of expressed proteins is shown. DOK1 protein level quantified from two independent immunoblots was normalized to the corresponding β-actin level (bottom). Fold induction is expressed relative to the baseline si-Luc. (C and D) Cells were transfected with si-E2F1 or si-Luc. At 24 h after transfection, the same cells were retransfected with the pCMV empty vector or pCMV-E2F1. The mRNA (C) and protein (D) expression levels of *E2F1* and *DOK1* were monitored by quantitative RT-PCR and immunoblotting. DOK1 protein levels from two independent immunoblots were quantified using ImageJ and normalized to the corresponding β-actin level (bottom). Fold induction is expressed relative to the baseline pCMV empty vector (bottom). (E) Cells were transfected with the indicated expression plasmids and analyzed by immunoblotting. The normalized relative level of DOK1 protein obtained from two independent immunoblots is shown (bottom).

the promoter region from bp −600 to −400, which contains only ERE1, has similar promoter activity to the 0.5-kb region containing the three binding sites and was strongly activated upon E2F1 expression (Fig. 1D, bottom). Moreover, a significant reduction in the promoter activity was observed when ERE1, ERE2, and ERE3 were individually or jointly mutated (Fig. 1E). In agreement with the data obtained with the deletion mutants, ERE1 mutation resulted in the greatest decrease in E2F1 *DOK1* promoter activation in the presence of endogenous or ectopically expressed E2F1 (Fig. 1E). Similar results were obtained in experiments using the 2.0-kb *DOK1* promoter in which the single EREs were mutated (data not shown). Together, these data indicate that the EREs, as identified in the region between bp −500 and +33 of the *DOK1* promoter, are the *cis* elements necessary for E2F1 to induce the highest *DOK1* promoter activity. In addition, the ERE1 located between bp −498 and −486 plays a major role in transcriptional regulation. However, our data suggest that E2F1 may also activate the *DOK1* promoter via a nonclassical canonical binding site. In

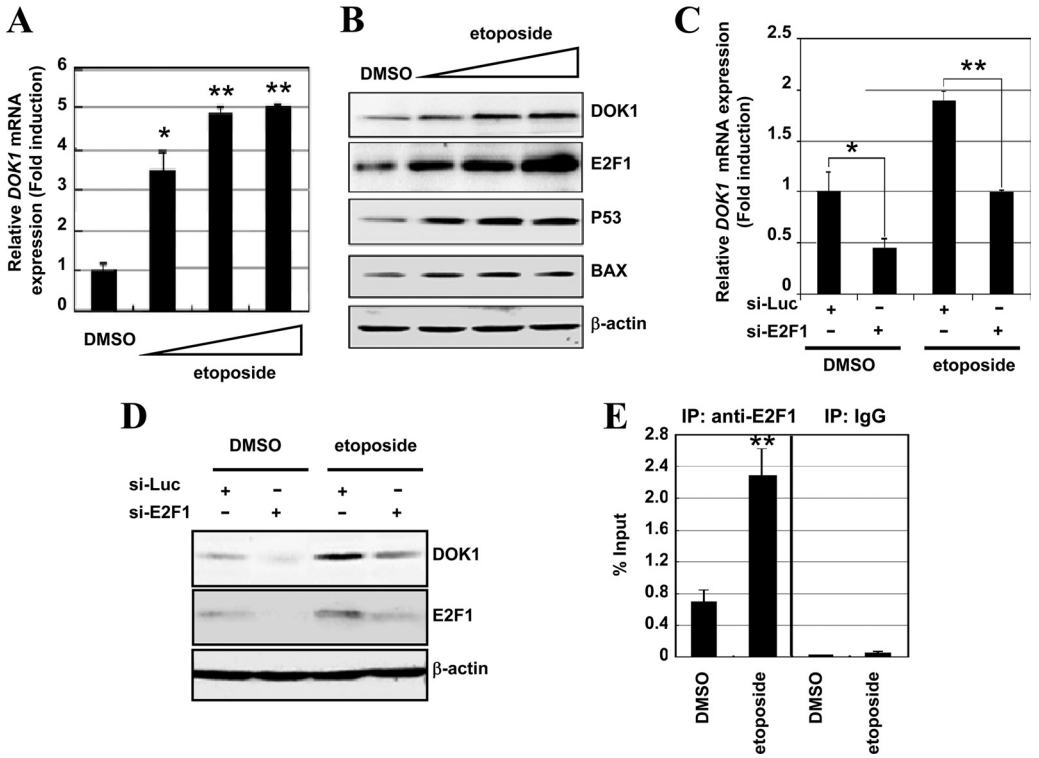

FIG 4 Etoposide treatment upregulates *DOK1* gene expression via E2F1. HEK293 cells were treated with 25, 50, or 100 μM etoposide or an equivalent volume of DMSO (as a control) for 24 h, and cells were then harvested for analysis. (A) mRNA levels of *DOK1* were measured by quantitative RT-PCR and normalized to the *GAPDH* mRNA level using the $\Delta\Delta C_T$ method. Fold induction is expressed relative to the baseline DMSO-treated cells. (B) Indicated proteins were detected by immunoblotting. (C) HEK293 cells were transfected with si-E2F1 or si-Luc (as a control). After 48 h, cells were treated with 50 μM etoposide or DMSO (control) for an additional 24 h. *DOK1* expression was measured by quantitative RT-PCR and normalized to the *GAPDH* level using the $\Delta\Delta C_T$ method. (D) Indicated proteins were detected by immunoblotting. (E) Quantitative ChIP analysis of E2F1 binding to the *DOK1* promoter ERE1 in HEK293 cells treated with 50 μM etoposide or an equivalent volume of DMSO (mock control) for 24 h. Data are presented as percentage of input. Error bars indicate the SD from three independent experiments performed in triplicate. Data were analyzed using Student's *t* test (*, $P < 0.05$; **, $P < 0.01$).

fact, E2F1 was still able to slightly stimulate the *DOK1* promoter in which all three E2F1 EREs were mutated (Fig. 1E). Accordingly, a reduction in E2F1-mediated *DOK1* promoter activity was observed when the region between bp −400 and −200, with no canonical E2F1 consensus binding sequences, was removed (Fig. 1D).

E2F1 is recruited to the *DOK1* promoter. Data obtained from the reporter assay suggested that E2F1 plays a key role in *DOK1* expression. Therefore, we investigated whether E2F1 is recruited to the *DOK1* promoter at ERE sites. To this end, we performed quantitative ChIP assays in HEK293 cells. The amplified promoter region of c-*FOS*, known to recruit E2F1 (30), was used as a positive control. As a negative control, a DNA segment upstream of the *DOK1* promoter (bp −1180 to −791) that lacks the putative binding sites for E2F1 was also included. Endogenous E2F1 was efficiently and specifically recruited to ERE1, with much less, if any, recruitment to ERE2 and ERE3 (Fig. 2A). Consistent with this observation, ectopic expression of E2F1 resulted in enhanced recruitment to the *DOK1* promoter, with a stronger affinity to ERE1 (Fig. 2A). To further corroborate our findings, we performed a new, modified ChIP assay, which monitors *in vivo* the E2F1 binding to transfected promoter fragments, as described by Wells and Farnham (29). In this assay, a single E2F1 core binding element was cloned in a luciferase reporter vector before transfection into HEK293 cells. To assess the recruitment of E2F1 *in vivo*, we then performed a quantitative ChIP assay using real-time PCR with specific primers within the reporter vector flanking the E2F1 core binding site. The empty vector and the cloned fragment from bp −1180 to −791 of the *DOK1* promoter that lacks the putative binding sites for E2F1 were used as negative controls. In agreement with previous data, we found that E2F1 is readily recruited to ERE1, ERE2, and ERE3, with a higher affinity for ERE1 (Fig. 2B). In addition, mutation in each of the three EREs dramatically decreased the recruitment of E2F1 (Fig. 2B). Consistent with these observations, ERE1, ERE2, and ERE3 in this new configuration were potent to activate the *DOK1* promoter (Fig. 2C), or to bind to E2F1 (Fig. 2D), in contrast to their respective mutants. Thus, E2F1 is efficiently recruited to the *DOK1* promoter region by mainly binding to ERE1.

It is noteworthy that binding sites of the E2F family members E2F2 and E2F3 were also found near the core sequence of E2F1 (Fig. 2E, top). However, in contrast to E2F1, both E2F2 and E2F3 were marginally recruited to their putative binding sites, with a slightly increased recruitment to E2F3 at site D (Fig. 2E). Thus, E2F2 and E2F3 have a limited role in *DOK1* gene expression, making E2F1 a major transcription factor controlling *DOK1* gene expression.

E2F1 positively regulates *DOK1* gene expression in cells. Because E2F1 is recruited directly to the *DOK1* promoter, where it mediates its activity, we investigated whether E2F1 binding to the

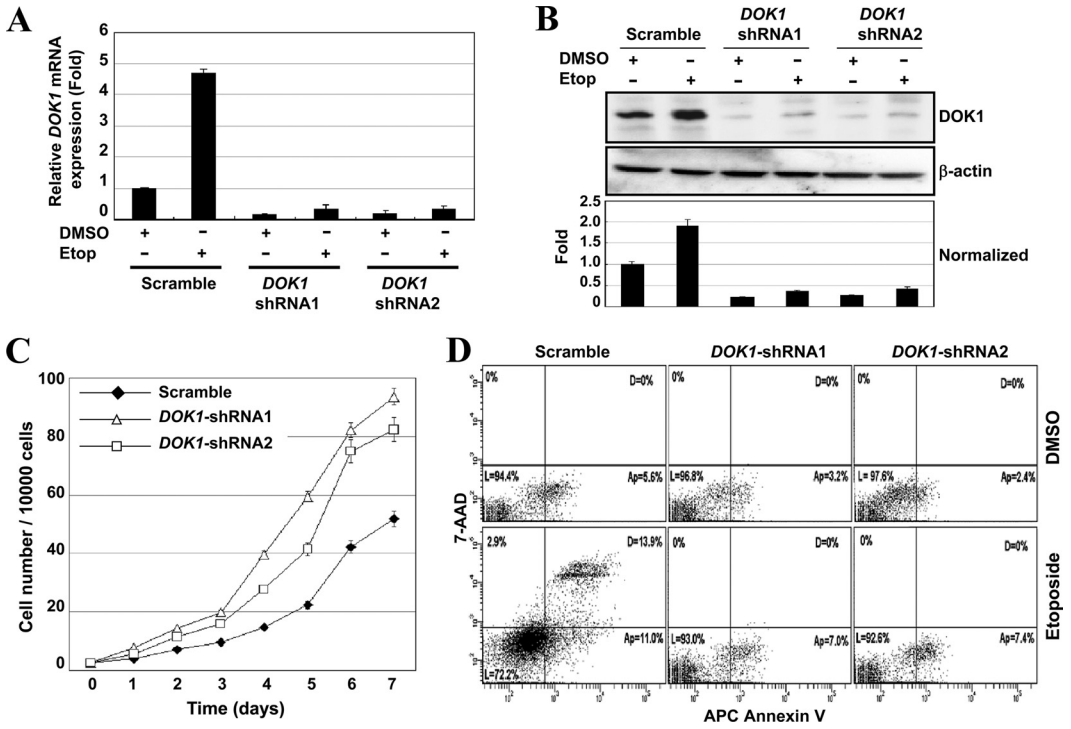

FIG 5 *DOK1* acts as a mediator of etoposide-induced apoptosis. HEK293 cells stably expressing scramble shRNA, *DOK1*-shRNA1, or *DOK1*-shRNA2 were treated with 50 μM etoposide or an equivalent volume of DMSO (mock control) for 24 h. (A) *DOK1* expression level was detected by RT-PCR. Values were normalized to the *GAPDH* expression level using the $\Delta\Delta C_T$ method. Fold induction is expressed relative to the baseline scramble mock-treated cells. (B) DOK1 protein level was detected by immunoblotting. A representative immunoblot is shown. Protein levels from two independent immunoblots were quantified using ImageJ and normalized to the corresponding β-actin level (bottom). Fold induction is expressed relative to the baseline scramble mock-treated cells. (C) HEK293 cells stably expressing scramble shRNA, *DOK1*-shRNA1, or *DOK1*-shRNA2 were monitored for cell proliferation. Data are representative of three independent experiments performed in duplicate. (D) Flow cytometry analysis of stained cells with APC annexin V and 7-amino-actinomycin D (7-AAD). Results are presented as dual-parameter scatter plots. Values indicate the percentage of living (L; annexin V^- and 7-AAD^-), early apoptotic (Ap; annexin V^+ and 7-AAD^-), and dead (D; annexin V^+ and 7-AAD^+) cells. A representative result of three independent experiments is shown.

DOK1 promoter leads to increased *DOK1* expression in cells. E2F1 was overexpressed in HEK293 cells, and the expression of the endogenous *DOK1* gene was determined by quantitative RT-PCR and immunoblotting. Ectopic expression of E2F1 resulted in a 3-fold increase in *DOK1* expression at both the mRNA (Fig. 3A) and protein (Fig. 3B) levels. Silencing the endogenous *E2F1* expression by 80% using siRNA-mediated knockdown resulted in a decrease of 70% in *DOK1* mRNA levels (Fig. 3A). Consistently, the decrease in the E2F1 protein level was also associated with a substantial reduction in the DOK1 protein level (Fig. 3B). Moreover, the rescue of E2F1 expression in HEK293 cells in which *E2F1* had been silenced led to a significant increase in endogenous *DOK1* at both the mRNA and protein levels (Fig. 3C and D). Furthermore, ectopic expression of a truncated form of E2F1 (E2F1, aa 1 to 374) that lacks the transactivation domain and acts as a dominant negative mutant also induced a substantial reduction in the DOK1 protein level (Fig. 3E). Taken together, these data further support that the transcription factor E2F1 is a major positive regulator of *DOK1* gene expression.

Etoposide treatment induces *DOK1* gene expression through E2F1. In addition to its positive regulatory role in cell proliferation, E2F1 has been found to be stabilized during cellular stresses, such as DNA damage induced by several chemical reagents, including etoposide (17). To evaluate whether activation of *DOK1* expression by E2F1 could be part of a cellular defense mechanism activated during cellular stress, we exposed cells to increasing concentrations of etoposide for 24 h. In agreement with previous findings (17), etoposide treatment resulted in the stabilization and accumulation of E2F1 protein (Fig. 4B). This process correlated with an increase in *DOK1* mRNA and protein levels (Fig. 4A and B). As a positive control, we also monitored the levels of the proapoptotic proteins p53 and BAX, known to be elevated upon etoposide treatment (Fig. 4B) (12, 21). Interestingly, E2F1 silencing dramatically reduced the accumulation of *DOK1* mRNA and protein levels induced by etoposide treatment (Fig. 4C and D). Quantitative ChIP assays also showed that etoposide-induced *DOK1* expression correlated with a significant recruitment of E2F1 to the *DOK1* promoter region ERE1 (Fig. 4E). Together, these data indicate that E2F1-induced *DOK1* expression is part of a cellular defense mechanism activated during cellular stress.

DOK1 inhibits cell growth and mediates etoposide-induced apoptosis. Given that *DOK1* expression is induced by a DNA damage agent such as etoposide, we investigated the physiological relevance of its functions in response to cellular stress. To address this issue, we established a stable cell line in which the expression of *DOK1* was significantly silenced (Fig. 5A and B). As reported previously (20, 23), inhibition of *DOK1* expression was associated with enhanced cell proliferation compared with control cells (Fig. 5C), consistent with its tumor suppressor functions (2, 8, 20, 24, 33). As expected, a high level of apoptosis occurs in cells exposed

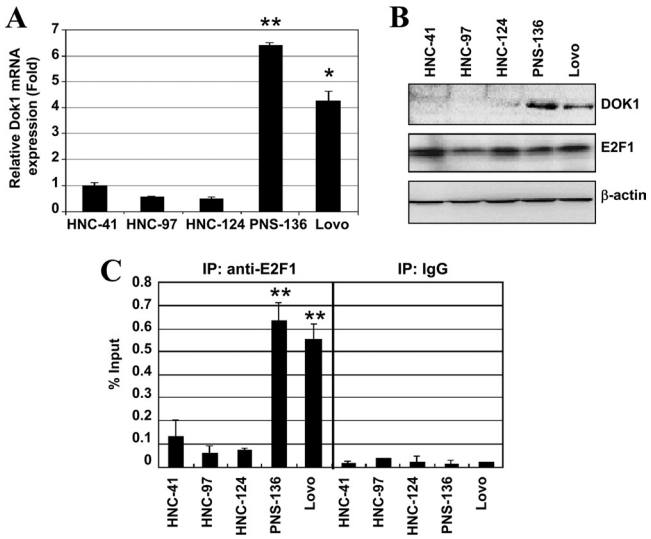

FIG 6 Loss of *DOK1* gene expression in HNC cell lines correlates with the lack of E2F1 recruitment to the *DOK1* promoter. HNC cell lines HNC-41, HNC-97, and HNC-124, as well as paranasal sinus cell line PNS-136 and colon cancer cell line LoVo, were cultured and used for different analyses. (A) The *DOK1* expression level was detected by RT-PCR. Values were normalized to the *GAPDH* expression level using the $\Delta\Delta C_T$ method. Fold induction is expressed relative to the HNC-41 cells. (B) Expression of the indicated proteins was monitored by immunoblotting. (C) Quantitative ChIP analysis of E2F1 recruitment to the *DOK1* promoter at ERE1 in the indicated cell lines. Data are presented as percentage of input. Error bars indicate the SD from three independent experiments performed in triplicate. Data were analyzed using Student's *t* test (*, $P < 0.05$; **, $P < 0.01$).

to etoposide in which *DOK1* is normally expressed (Fig. 5D, Scramble). In contrast, knocking down *DOK1* by two independent shRNAs resulted in a very low level of apoptosis after exposure to etoposide (Fig. 5D, *DOK1*-shRNA1 and *DOK1*-shRNA2). Taken together, these data suggest that DOK1 plays a key role in the control of cell proliferation and acts as a key factor in etoposide-induced apoptosis.

DOK1 expression silencing in HNC cell lines correlates with a decreased recruitment of E2F1 to the *DOK1* promoter. We recently reported that the *DOK1* gene is silenced in HNC cell lines and in a variety of primary human tumors, as a result of hypermethylation of its promoter region (24). As E2F1 appears to play a major role in the regulation of *DOK1* expression, we determined whether its role in controlling *DOK1* expression is compromised in HNC cells. Indeed, the lack of *DOK1* expression in these cells could be the consequence of a low level of E2F1, or its inability to be efficiently recruited to the *DOK1* promoter. We first confirmed that E2F1 is expressed in HNC cell lines and that *DOK1* is weakly expressed in HNC-41, HNC-97, and HNC-124 cells compared with PNS-136 and LoVo cells, which were previously characterized for *DOK1* expression (Fig. 6A and B) (24). Quantitative ChIP assays showed that in the DOK1-expressing cell lines PNS-136 and LoVo, E2F1 was recruited efficiently to the *DOK1* promoter (ERE1), whereas E2F1 was found to be weakly associated with the *DOK1* promoter in the DOK1-negative cell lines HNC-41, HNC-97, and HNC-124 (Fig. 6C). Thus, the loss of *DOK1* expression in the HNC-41, HNC-97, and HNC-124 cell lines correlates with a lack of E2F1 recruitment to the *DOK1* promoter. However, the possible inactivation of other transcription factors as a result of epigenetic modifications cannot be completely excluded.

5′-aza treatment affects DNA methylation and chromatin remodeling to mediate E2F1 recruitment and *DOK1* expression in HNC cells. Since the *DOK1* gene is hypermethylated in HNC cell lines (24), we checked the methylation level in CpGs specifically within the region of ERE1, the binding motif showing the highest affinity for E2F1. We indeed found that E2F1 recruitment to ERE1 inversely correlates with the methylation level of the CpGs within ERE1 in these cell lines (Fig. 6C and 7A). Therefore, we investigated the effect of DNA demethylation on the recruitment of E2F1 to the *DOK1* promoter region. HNC cell lines were treated with the methyltransferase inhibitor 5′-aza, followed by *DOK1* expression monitoring. As expected, 5′-aza treatment led to an increase in *DOK1* gene expression at the mRNA and protein levels (Fig. 7B and C). This event correlates with a significant increase in E2F1 recruitment to ERE1 of the *DOK1* promoter (Fig. 7D), where ERE1 CpGs were notably less methylated upon 5′-aza exposure (Fig. 7E). Thus, the aberrant hypermethylation of the *DOK1* promoter in HNC cell lines likely hampers the recruitment of E2F1 to its binding site in the *DOK1* promoter region and compromises *DOK1* expression. To further support this observation, we performed *in vitro* methylation of the *DOK1* promoter with M.SssI methylase and monitored its transcriptional activity in the presence of ectopically expressed E2F1. We confirmed by bisulfite PCR sequencing that M.SssI efficiently methylates the CpG sequence within the ERE sites (Fig. 7F). In agreement with previous findings, methylation of ERE sites significantly interferes with E2F1 binding (Fig. 7G) and blocks the activity of the *DOK1* promoter in cells expressing endogenous or ectopic E2F1 (Fig. 7H). These data indicate that DNA methylation can impair E2F1 recruitment to the *DOK1* promoter *in vitro*, which correlates with the loss of its transcriptional activity and can impair *DOK1* expression in cancer cells.

Because 5′-aza appears to affect both DNA methylation and chromatin remodeling in cells, the two key events in the regulation of gene expression (28, 35), we investigated whether histone modifications could also play a role in 5′-aza-induced E2F1 recruitment to the *DOK1* promoter in HNC cells. To this end, we evaluated the levels of different epigenetic markers on the *DOK1* promoter of HNC cells, including H3K9 acetylation and H3K4 trimethylation (epigenetic markers for transcriptional activation) and H3K27 trimethylation, a key marker for epigenetic repression that often precedes DNA methylation (26). We found that repression of *DOK1* expression in HNC cells correlated with low levels of H3K9 acetylation and H3K4 trimethylation in the *DOK1* promoter, but with a significant increase in H3K27 trimethylation (Fig. 8A, black bars). Conversely, induction of *DOK1* expression after 5′-aza treatment correlated with a significant increase in H3K9 acetylation and H3K4 trimethylation at the *DOK1* promoter and a lower level of H3K27 trimethylation (Fig. 8A, white bars). These findings are consistent with the data obtained in the PNS-136 cell line used as a control, in which *DOK1* is normally expressed. In this cell line, the presence or absence of 5′-aza did not change the high levels of H3K9 acetylation and H3K4 trimethylation on the *DOK1* promoter compared with HNC-41, HNC-97, and HNC-124 cells, and consistently, H3K27 trimethylation was maintained at a low level regardless of 5′-aza treatment (Fig. 8A). Taken together, these results, along with those described above, indicate that E2F1 recruitment to the *DOK1* promoter in 5′-aza-treated cells is a combined result of DNA demeth-

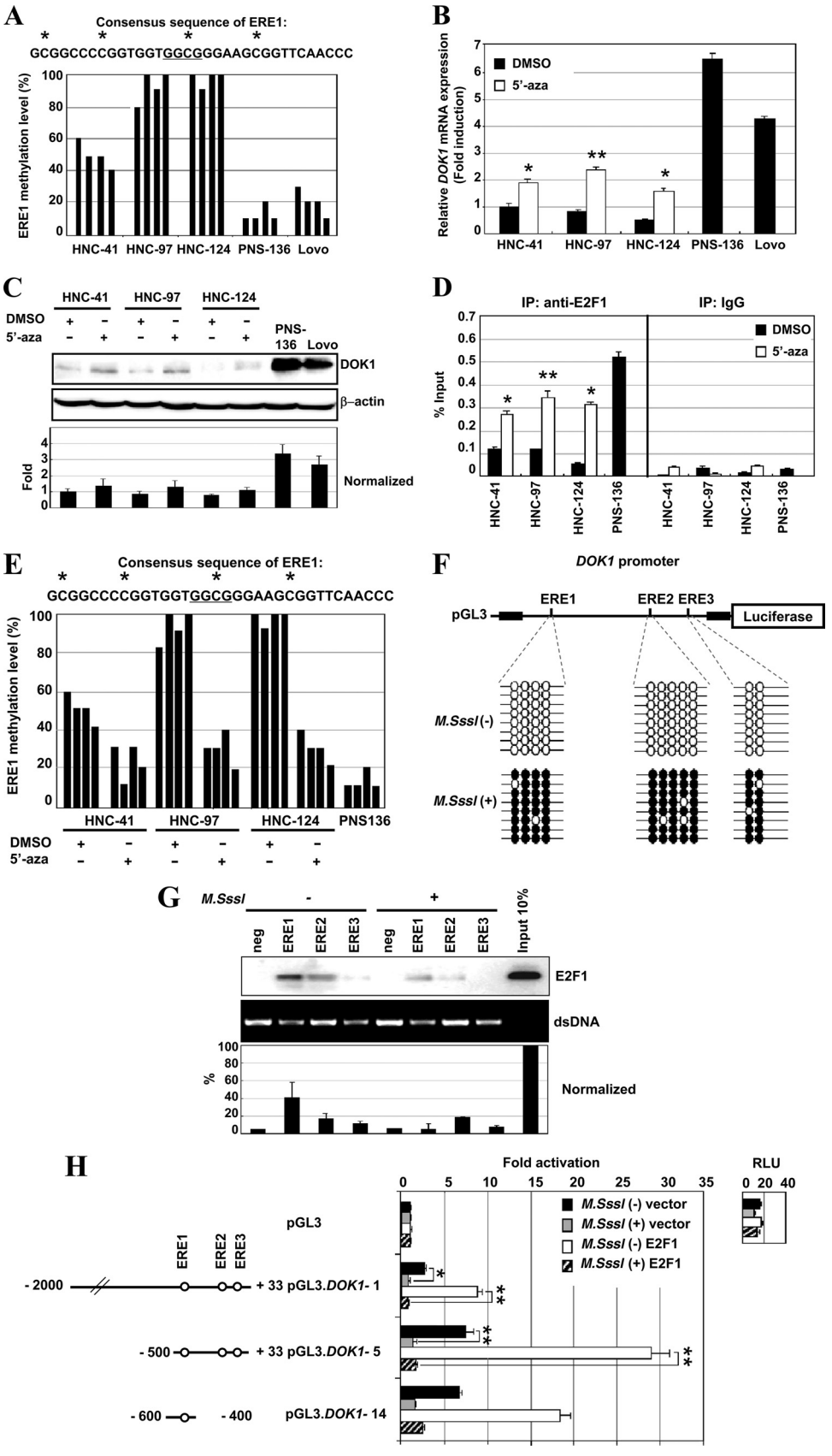
A
Consensus sequence of ERE1:
GCGGCCCCGGTGGTGGCGGGAAGCGGTTCAACCC
ERE1 methylation level (%)
HNC-41 HNC-97 HNC-124 PNS-136 Lovo
B
Relative DOK1 mRNA expression (Fold induction)
DMSO
5'-aza
HNC-41 HNC-97 HNC-124 PNS-136 Lovo
C
HNC-41 HNC-97 HNC-124
DMSO
5'-aza
PNS-136 Lovo
DOK1
β–actin
Fold
Normalized
D
IP: anti-E2F1
IP: IgG
% Input
DMSO
5'-aza
HNC-41 HNC-97 HNC-124 PNS-136
E
Consensus sequence of ERE1:
GCGGCCCCGGTGGTGGCGGGAAGCGGTTCAACCC
ERE1 methylation level (%)
HNC-41 HNC-97 HNC-124 PNS136
DMSO
5'-aza
F
DOK1 promoter
pGL3
ERE1
ERE2 ERE3
Luciferase
M.SssI (-)
M.SssI (+)
G
M.SssI
neg ERE1 ERE2 ERE3 neg ERE1 ERE2 ERE3 Input 10%
E2F1
dsDNA
%
Normalized
H
Fold activation
RLU
M.SssI (-) vector
M.SssI (+) vector
M.SssI (-) E2F1
M.SssI (+) E2F1
pGL3
ERE1 ERE2 ERE3
- 2000
+ 33 pGL3.DOK1- 1
- 500
+ 33 pGL3.DOK1- 5
- 600
- 400
pGL3.DOK1- 14

ylation and chromatin remodeling for the recruitment of E2F1 and the expression of *DOK1*.

It is not clear whether the recruitment of E2F1 to the *DOK1* promoter in these cells is the only factor responsible for the increased level of *DOK1* after 5′-aza treatment. To address this issue, we knocked down E2F1 expression in HNC-41, HNC-124, and PNS-136 cells and monitored *DOK1* expression after 5′-aza treatment. As expected, exposure of HNC-41 and HNC-124 cells transduced with scramble oligonucleotide (control) to 5′-aza resulted in an increased *DOK1* expression at both the mRNA and protein levels (Fig. 8B and C). The treatment did not affect the level of *DOK1* expression in PNS-136 control cells, in which *DOK1* is constitutively expressed (Fig. 8B and C). Most importantly, the inhibition of E2F1 expression in HNC-41and HNC-124 cells resulted in a decrease of *DOK1* expression levels, indicating that E2F1 plays a critical role in controlling *DOK1* expression in these cancer cells. Interestingly, exposure to 5′-aza did not result in a significant increase in *DOK1* expression in these cells when E2F1 expression was inhibited (Fig. 8B and C). Furthermore, a strong reduction in *DOK1* expression occurred in PNS-136 control cells when E2F1 expression was compromised (Fig. 8B and C). Taken together, these findings and the data reported above demonstrate that E2F1 is the major transcription factor that is mobilized for *DOK1* expression after 5′-aza treatment and plays a critical role in the regulating *DOK1* expression in HNC cells.

Effects of etoposide on *DOK1* expression in HNC cell lines. Etoposide treatment of HEK293 cells led to an increase of *DOK1* expression and apoptosis (Fig. 4 and 5). It is not known whether etoposide can induce *DOK1* expression in HNC cells, where the *DOK1* promoter is methylated and eventually promotes cell death. To address this issue, we treated HNC-41 and HNC-124 cells with different concentrations of etoposide and monitored the DOK1 protein level. We also evaluated the percentages of early apoptotic and dead cells under these conditions. HEK293 cells, in which *DOK1* is constitutively expressed, were used as a control. Consistent with previous data (Fig. 5D), etoposide induced a significant increase in the DOK1 protein level in HEK293 cells (Fig. 9A). However, in contrast, etoposide did not induce *DOK1* expression in HNC-41 and HNC-124 cells, in which *DOK1* expression is silenced as a result of hypermethylation of its promoter (Fig. 9A). Accordingly, etoposide led to an increased level of apoptosis in HEK239 but not in HNC-41 and HNC-124 cells (Fig. 9B). In summary, these results provide further evidence for the role of DOK1 in regulating cell stress-induced apoptosis.

DISCUSSION

Several independent studies by our group and others have highlighted the tumor suppressor role of DOK1. In addition to its ability to inhibit cell proliferation and MAP kinase activity, DOK1 suppresses cell transformation and tumor growth in various experimental systems (8, 10, 23, 33). The *DOK1* gene was found to be mutated in CLL (16) and to be silenced in various human cancers, including HNC, lung and liver cancers, and lymphoma, by hypermethylation of its promoter region (14, 24). Moreover, independent animal studies and analysis of human tumor samples have demonstrated the tumor suppressor role of *DOK1* and its related family member *DOK2* in lung cancer and histiocytic sarcoma (2, 19). Deciphering how *DOK1* gene expression is regulated, particularly in relation to its inactivation by promoter methylation, is important to better understand the role of *DOK1* in human cancer development. Despite the extensive studies on the biological properties of DOK1, very little is known about the mechanisms involved in the transcriptional regulation of the *DOK1* gene. In this study, we characterized the *DOK1* promoter and demonstrated the key role of E2F1 in activating *DOK1* expression. We identified three E2F response elements, but one located between bp −498 and −486 (ERE1) appears to be the main element that mediates E2F-driven transcription. These conclusions are based on data obtained from a broad range of experiments in different *in vitro* models, including reporter gene assays and quantitative ChIP experiments that analyzed endogenous events. E2F1 acts mainly as a transcriptional activator. It has been demonstrated to have a dual functionality in promoting proliferation by regulating genes controlling cell cycle progression and DNA synthesis, e.g., cyclins and c-*Myc* (6) and, conversely, by playing an antiproliferative role in response to cellular stress (17) by regulating tumor suppressor and proapoptotic genes, e.g., *RB1*, *p14ARF*, and *TP73* (25, 27, 37).

Here, we showed for the first time that *DOK1* expression is induced in the presence of cellular stresses, e.g., induced DNA damage. Indeed, etoposide treatment promoted E2F1 accumulation and, consequently, *DOK1* promoter activation. Thus, *DOK1*,

FIG 7 5′-Aza-2′-deoxycytidine (5′-aza) treatment rescues the recruitment of E2F1 to the *DOK1* promoter in HNC cells. (A) DNA methylation levels of ERE1 CpGs in HNC cell lines, PNS-136, and LoVo were measured by bisulfite sequencing PCR using 10 clones from each cell line. Asterisks indicate the methylated CpG sites. The ERE1 core sequence is underlined. Each bar represents the results obtained for an individual CpG site. (B) HNC cells were treated with 30 μM 5′-aza or DMSO for 4 days, and cells were then harvested for *DOK1* mRNA expression detection by RT-PCR. Values were normalized to the *GAPDH* expression level using the $\Delta\Delta C_T$ method. Fold induction is expressed relative to the HNC-41 cells treated with DMSO. (C) Expression of proteins was detected by immunoblotting. A representative result from two independent experiments is shown. Protein levels from two independent immunoblots were quantified using ImageJ and normalized to the corresponding β-actin level (bottom). Fold induction is expressed relative to HNC-41 cells treated with DMSO. (D) Quantitative ChIP analysis of E2F1 recruitment to ERE1 of the *DOK1* promoter. Data are presented as percentage of input. Error bars indicate the SD from three independent experiments performed in triplicate. Data were analyzed using Student's *t* test (*, $P < 0.05$; **, $P < 0.01$). (E) DNA methylation levels of ERE1 CpGs from HNC cell lines and PNS-136 treated with 5′-aza or DMSO were measured by bisulfite sequencing PCR using 10 clones from each condition. Each bar represents the methylation levels obtained for an individual CpG site. (F) Schematic representation of the *DOK1* promoter methylation status from multiple individual clones derived by PCR on bisulfite-treated pGL3-*DOK1*-5 reporter plasmid. Black circles represent methylated CpG sites, and white circles represent unmethylated CpG sites. Each horizontal line represents an individual allele. (G) *In vitro* DNA pulldown assay. EREs were amplified by PCR using 5′-biotinylated primers and then treated with or without M.SssI methylase. The oligonucleotides were incubated with total lysate from E2F1-overexpressing HEK293 cells, and a pulldown assay was performed using streptavidin-agarose beads. Immunoblotting was used to check the recruitment of E2F1 to the different PCR fragments. A representative immunoblot is shown. E2F1 protein bands from three independent experiments were quantified using ImageJ software, and the values were normalized to the PCR products used in each experiment and checked on agarose gel (double-stranded DNA). (H) HEK293 cells were cotransfected together with the *Renilla* plasmid (used as an internal control for transfection), the pGL3-*DOK1*-1, -5, and -14 constructs treated with or without M.SssI methylase, along with the E2F1-expressing plasmid or vector (control). At 48 h after transfection, luciferase activity was measured. Results (±SD) are representative of three independent experiments performed in triplicate. Data were analyzed using Student's *t* test (*, $P < 0.05$; **, $P < 0.01$).

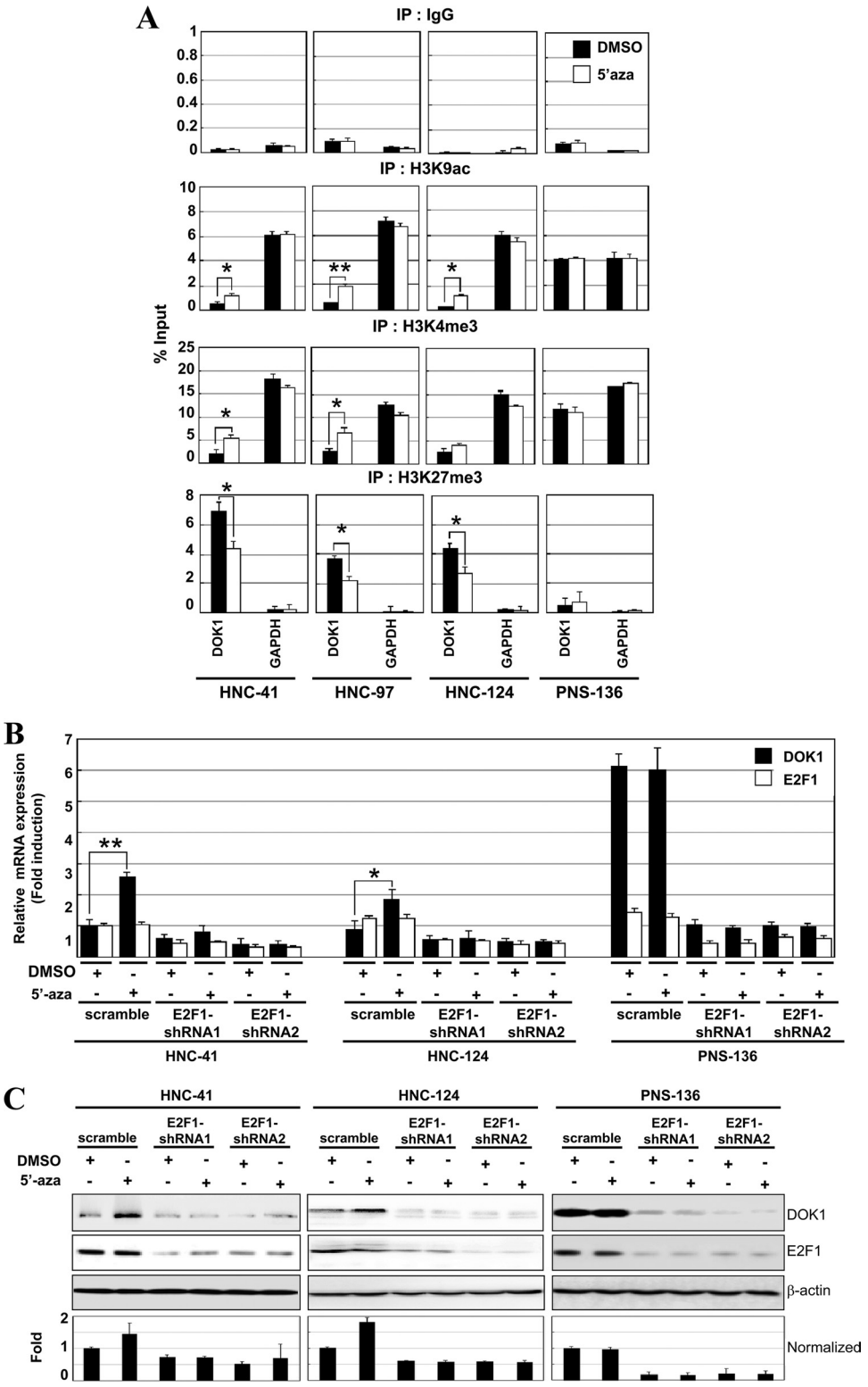

FIG 8 Chromatin remodeling in 5′-aza-induced *DOK1* expression and critical role of E2F1 in controlling *DOK1* expression in HNC cells. (A) HNC-41, HNC-97, HNC-124, and PNS-136 cells treated with 5′-aza or DMSO were subjected to quantitative ChIP analysis for the indicated histone modifications. The *DOK1* promoter and *GAPDH* were amplified by RT-PCR. Data are presented as percentages of input. Error bars indicate the SD from two independent experiments performed in triplicate. Data were analyzed using Student's *t* test (*, $P < 0.05$; **, $P < 0.01$). (B) HNC-41, HNC-124, and PNS-136 cells stably expressing scramble, *E2F1*-shRNA1, or *E2F1*-shRNA2 were treated with 5′-aza or DMSO (mock) for 4 days. Cells were then analyzed for *DOK1* and *E2F1* expression by real-time PCR. Values from two independent experiments were normalized to the *GAPDH* expression level using the $\Delta\Delta C_T$ method. Fold induction is expressed relative to the HNC-41 cells treated with DMSO. Data were analyzed using Student's *t* test (*, $P < 0.05$; **, $P < 0.01$). (C) Expression of proteins was detected by immunoblotting. A representative blot from two independent experiments is shown. Protein levels from two independent immunoblots were quantified using ImageJ and normalized to the corresponding β-actin level (bottom). Fold induction is expressed relative to cells treated with DMSO.

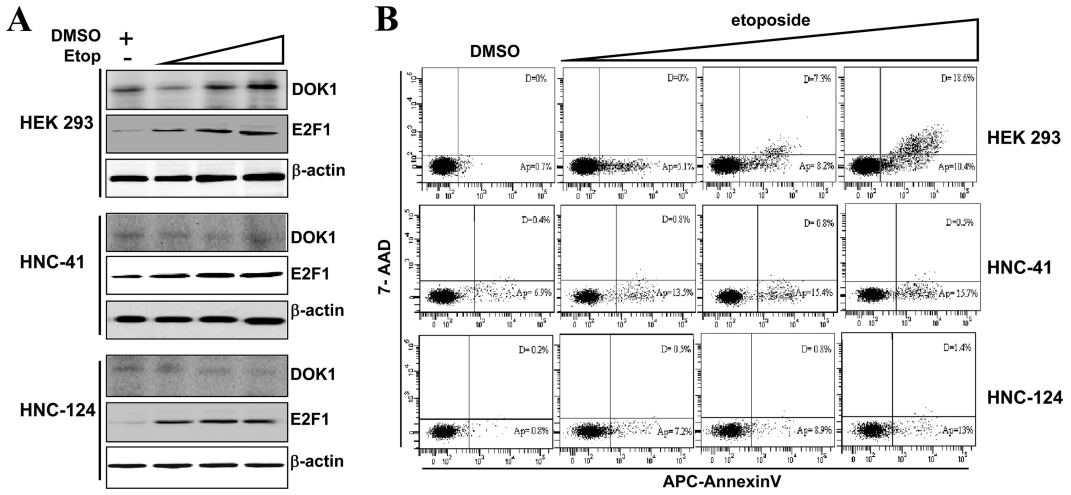

FIG 9 Effects of etoposide on DOK1 expression in HNC cells. HEK293 cells and HNC-41 and HNC-124 cells were treated with 25, 50, or 100 μM etoposide or an equivalent volume of DMSO (as a control) for 24 h, and cells were then harvested for analysis. (A) The indicated proteins were detected by immunoblotting. (B) Etoposide-induced apoptosis was monitored by flow cytometry analysis of stained cells with APC annexin V and 7-AAD. Results are presented as dual-parameter scatter plots. Values indicate the percentages of early apoptotic (Ap; annexin V^+ and 7-AAD^-) and dead (D; annexin V^+ and 7-AAD^+) cells.

similarly to *TP73*, is a newly discovered E2F1 target whose transcriptional activation appears to be part of a safeguard mechanism activated during unrestricted cell proliferation and/or DNA damage. Consistent with this observation, silencing of *DOK1* through interference RNA promotes cell proliferation and protects against apoptosis after DNA damage. Interestingly, HNC cells, in which the *DOK1* promoter is methylated, do not accumulate DOK1 and undergo apoptosis upon exposure to etoposide (Fig. 9). This event is likely due to the inability of etoposide to alleviate *DOK1* promoter methylation and to promote chromatin remodeling. Taken together, these findings further confirm the important role of DOK1 in mediating cellular stress-induced apoptosis.

The mechanisms underlying DOK1-mediated apoptosis induced by DNA damage remain to be elucidated. It is likely that DOK1 promotes etoposide-induced apoptosis by inhibiting MAP kinase activation and downregulating survival proteins. Indeed, it has been reported that DOK1 mediates activin-induced apoptosis via the activin receptors/Smad axis by suppressing MAP kinase activation and inhibiting Bcl-X_L expression (32). Thus, DOK1 appears to play a pivotal role in mediating apoptosis induced by different agents.

Our group previously showed that loss of *DOK1* expression is often observed in a variety of human cancers and is invariably due to hypermethylation of its promoter region (1, 14, 24). DNA methylation is thought to silence gene expression either by directly impeding transcription factor binding or by recruiting other proteins, known as methyl-CpG-binding domain proteins (MBDs), histone deacetylases (HDACs), and other chromatin remodeling proteins (4, 13). Thereby, these recruited complexes promote the formation of compact, inactive chromatin that is inaccessible to transcription factors. The data presented here not only corroborate these previous findings but also elucidate the mechanism of this event. We clearly demonstrated that DNA methylation does indeed impair the recruitment of E2F1 to the *DOK1* promoter and leads to *DOK1* promoter inactivation and gene silencing. In addition to DNA methylation, we observed that levels of histone H3K9 acetylation and H3K4 trimethylation, markers for active transcription, were greatly reduced in HNC cells, which correlates with *DOK1* silencing (Fig. 8A). Interestingly, the level of H3K27 trimethylation, a marker for gene repression, was higher in these cells, which corroborates the silencing through DNA methyltransferases (DNMTs) in these cells (Fig. 8A). The finding that 5′-aza treatment increased *DOK1* expression in HNC cells revealed that this agent indeed plays a pleiotropic role in activating the expression of epigenetically silenced genes through DNA demethylation and chromatin remodeling via differential specific histone modifications. Indeed, here we show that, in addition to its effects in inhibiting DNA methylation, 5′-aza significantly increased the level of H3K9 acetylation and H3K4 trimethylation at the *DOK1* promoter and decreased the level of H3K27 trimethylation (Fig. 8A, white bars). These chromatin-remodeling events converge to modify the nucleosome structure into an open conformation, making the region more accessible to E2F1 to drive *DOK1* expression. Interestingly, inhibiting E2F1 expression in HNC cells hampers the reactivation of *DOK1* expression induced by 5′-aza (Fig. 8B and C), supporting the critical role of E2F1 in regulating DOK1 expression. Even though our data support that E2F1 is a major transcription factor that regulates *DOK1* expression, the role of other transcription factors such as RXRs cannot be completely excluded. However, the potential role of these transcription factors should be relatively limited, as they are unable to significantly promote *DOK1* expression in the absence of E2F1, even under conditions where the *DOK1* promoter is fully accessible.

In conclusion, our findings revealed a key role of E2F1 in the regulation of *DOK1* expression in relation to human cancer development. These findings could ultimately define *DOK1* as a potentially useful biomarker for cancer screening and therapeutic approaches.

ACKNOWLEDGMENTS

We thank Kristian Helin, Tom Gilmore, Guntram Suske, and Pierre Hainaut for reagents and Karen Muller for editing. We also thank Cyrille

Cuenin, Claudia Zannetti, and all members of the Infections and Cancer Biology Group for their contributions.

M.S. and R.S. were supported by the IARC Fellowship Program. This work was partially supported by grants from La Ligue Régionale de Lutte contre le Cancer du Rhône et de la Drôme (to B.S.S.).

REFERENCES

1. **Balassiano K, et al.** 2011. Aberrant DNA methylation of cancer-associated genes in gastric cancer in the European Prospective Investigation into Cancer and Nutrition (EPIC-EURGAST). Cancer Lett. **311**:85–95.
2. **Berger AH, et al.** 2010. Identification of DOK genes as lung tumor suppressors. Nat. Genet. **42**:216–223.
3. **Bird A.** 2002. DNA methylation patterns and epigenetic memory. Genes Dev. **16**:6–21.
4. **Bogdanovic O, Veenstra GJ.** 2009. DNA methylation and methyl-CpG binding proteins: developmental requirements and function. Chromosoma **118**:549–565.
5. **Carpino N, et al.** 1997. p62(dok): a constitutively tyrosine-phosphorylated, GAP-associated protein in chronic myelogenous leukemia progenitor cells. Cell **88**:197–204.
6. **DeGregori J, Kowalik T, Nevins JR.** 1995. Cellular targets for activation by the E2F1 transcription factor include DNA synthesis- and G1/S-regulatory genes. Mol. Cell. Biol. **15**:4215–4224.
7. **DeGregori J, Leone G, Miron A, Jakoi L, Nevins JR.** 1997. Distinct roles for E2F proteins in cell growth control and apoptosis. Proc. Natl. Acad. Sci. U. S. A. **94**:7245–7250.
8. **Di Cristofano A, et al.** 2001. p62(dok), a negative regulator of Ras and mitogen-activated protein kinase (MAPK) activity, opposes leukemogenesis by p210(bcr-abl). J. Exp. Med. **194**:275–284.
9. **Gong Y, et al.** 2006. NSPc1 is a cell growth regulator that acts as a transcriptional repressor of p21Waf1/Cip1 via the RARE element. Nucleic Acids Res. **34**:6158–6169.
10. **Hosooka T, et al.** 2001. Inhibition of the motility and growth of B16F10 mouse melanoma cells by dominant negative mutants of Dok-1. Mol. Cell. Biol. **21**:5437–5446.
11. **Inaba T, et al.** 1991. Philadelphia chromosome positive precursor B-cell acute lymphoblastic leukemia with a translocation t(2;14)(p13;q32). Leukemia **5**:719–722.
12. **Karpinich NO, Tafani M, Rothman RJ, Russo MA, Farber JL.** 2002. The course of etoposide-induced apoptosis from damage to DNA and p53 activation to mitochondrial release of cytochrome c. J. Biol. Chem. **277**: 16547–16552.
13. **Klose RJ, Bird AP.** 2006. Genomic DNA methylation: the mark and its mediators. Trends Biochem. Sci. **31**:89–97.
14. **Lambert MP, et al.** 2011. Aberrant DNA methylation distinguishes hepatocellular carcinoma associated with HBV and HCV infection and alcohol intake. J. Hepatol. **54**:705–715.
15. **Lamkin TJ, Chin V, Yen A.** 2006. All-trans retinoic acid induces p62DOK1 and p56DOK2 expression which enhances induced differentiation and G0 arrest of HL-60 leukemia cells. Am. J. Hematol. **81**:603–615.
16. **Lee S, et al.** 2004. Frameshift mutation in the Dok1 gene in chronic lymphocytic leukemia. Oncogene **23**:2287–2297.
17. **Lin WC, Lin FT, Nevins JR.** 2001. Selective induction of E2F1 in response to DNA damage, mediated by ATM-dependent phosphorylation. Genes Dev. **15**:1833–1844.
18. **Mashima R, Hishida Y, Tezuka T, Yamanashi Y.** 2009. The roles of Dok family adapters in immunoreceptor signaling. Immunol. Rev. **232**:273–285.
19. **Mashima R, et al.** 2010. Mice lacking Dok-1, Dok-2, and Dok-3 succumb to aggressive histiocytic sarcoma. Lab. Invest. **90**:1357–1364.
20. **Mercier PL, et al.** 2011. Characterization of DOK1, a candidate tumor suppressor gene, in epithelial ovarian cancer. Mol. Oncol. **5**:438–453.
21. **Miao L, Yi P, Wang Y, Wu M.** 2003. Etoposide upregulates Bax-enhancing tumour necrosis factor-related apoptosis inducing ligand-mediated apoptosis in the human hepatocellular carcinoma cell line QGY-7703. Eur. J. Biochem. **270**:2721–2731.
22. **Nelms K, Snow AJ, Noben-Trauth K.** 1998. Dok1 encoding p62(dok) maps to mouse chromosome 6 and human chromosome 2 in a region of translocation in chronic lymphocytic leukemia. Genomics **53**:243–245.
23. **Niki M, et al.** 2004. Role of Dok-1 and Dok-2 in leukemia suppression. J. Exp. Med. **200**:1689–1695.
24. **Saulnier A, et al.** 2012. Inactivation of the putative suppressor gene DOK1 by promoter hypermethylation in primary human cancers. Int. J. Cancer **130**:2484–2494.
25. **Shan B, Chang CY, Jones D, Lee WH.** 1994. The transcription factor E2F-1 mediates the autoregulation of RB gene expression. Mol. Cell. Biol. **14**:299–309.
26. **Simon JA, Lange CA.** 2008. Roles of the EZH2 histone methyltransferase in cancer epigenetics. Mutat. Res. **647**:21–29.
27. **Urist M, Tanaka T, Poyurovsky MV, Prives C.** 2004. p73 induction after DNA damage is regulated by checkpoint kinases Chk1 and Chk2. Genes Dev. **18**:3041–3054.
28. **Villa R, et al.** 2007. Role of the polycomb repressive complex 2 in acute promyelocytic leukemia. Cancer Cell **11**:513–525.
29. **Wells J, Farnham PJ.** 2002. Characterizing transcription factor binding sites using formaldehyde crosslinking and immunoprecipitation. Methods **26**:48–56.
30. **Wells J, Graveel CR, Bartley SM, Madore SJ, Farnham PJ.** 2002. The identification of E2F1-specific target genes. Proc. Natl. Acad. Sci. U. S. A. **99**:3890–3895.
31. **Woodring PJ, et al.** 2004. c-Abl phosphorylates Dok1 to promote filopodia during cell spreading. J. Cell Biol. **165**:493–503.
32. **Yamakawa N, Tsuchida K, Sugino H.** 2002. The rasGAP-binding protein, Dok-1, mediates activin signaling via serine/threonine kinase receptors. EMBO J. **21**:1684–1694.
33. **Yasuda T, et al.** 2004. Role of Dok-1 and Dok-2 in myeloid homeostasis and suppression of leukemia. J. Exp. Med. **200**:1681–1687.
34. **Yoffe G, Howard-Peebles PN, Smith RG, Tucker PW, Buchanan GR.** 1990. Childhood chronic lymphocytic leukemia with (2;14) translocation. J. Pediatr. **116**:114–117.
35. **Yun J, et al.** 2012. Gene silencing of EREG mediated by DNA methylation and histone modification in human gastric cancers. Lab. Invest. **92**:1033–1044.
36. **Zannetti C, et al.** 2010. C/EBP{delta} and STAT-1 are required for TLR8 transcriptional activity. J. Biol. Chem. **285**:34773–34780.
37. **Zhang HJ, et al.** 2009. 8-Chloro-adenosine-induced E2F1 promotes p14ARF gene activation in H1299 cells through displacing Sp1 from multiple overlapping E2F1/Sp1 sites. J. Cell Biochem. **106**:464–472.